ARTICLE

Visualization of Melting of Antiferromagnetic Insulator Phase in Phase-Separated Manganite Film using Magnetic Force Microscopy

Hai-biao Zhou[a,b], Yu-bin Hou[b], Qing-you Lu[a,b*]

a. Hefei National Laboratory for Physical Sciences at the Microscale, University of Science and Technology of China, Hefei 230026, China
b. High Magnetic Field Laboratory, Chinese Academy of Sciences and University of Science and Technology of China, Hefei 230031, China

(Dated: Received on April 11, 2015; Accepted on May 24, 2015)

The phase separation and magnetic-field-induced transition of the antiferromagnetic charge-ordered insulator (AFI) phase into the ferromagnetic metal (FM) phase in an anisotropically-strained manganite thin film is directly imaged using a home-built magnetic force microscope (MFM). The MFM images at 10 K show that the two competing phases already coexist in zero magnetic field. Remarkably anisotropic distribution of the stripe-like phase domains are observed, which can qualitatively account for the anisotropic transport. Above 2.2 T, the AFI phase starts to transform into FM phase gradually. The melting of AFI phase is completed at 3.2 T. The FM phase can be retained after the magnetic field is removed, suggesting the metastable nature of the AFI phase at this temperature.

Key words: Manganite, Phase-separation, Phase transition, Magnetic force microscope

I. INTRODUCTION

The phase separation involving competing phases has been a central topic in the physics of perovskite manganties showing colossal magnetoresistance [1]. The phase separation can be induced by strain interactions [2]. The elastic epitaxial strain can play an essential role in the phase separation and physical properties of manganites films. One example is that when deposited on $LaAlO_3$ substrate, a charge-ordered insulator ground state can be induced even in the $La_{0.67}Ca_{0.33}MnO_3$ (LCMO) thin film, which is doped nearly at the optimal level for a ferromagnetic ground state in the bulk form [3]. Besides, the charge-ordering transition in $Nd_{1/2}Sr_{1/2}MnO_3$ is lost when deposited on $SrTiO_3$ (100) or (111) substrate, while it can be observed when deposited on $SrTiO_3$(110) substrate [4]. In addition, the elastic epitaxial strain has profound effects on the microscopic structures of phase separation. For example, conducting resistance network along the crystalline axes and anisotropic phase domains have been observed in $Nd_{1/2}Sr_{1/2}MnO_3$ and $La_{0.325}Pr_{0.3}Ca_{0.375}MnO_3$ thin films [5, 6], respectively, with the latter one qualitatively explaining the resistivity anisotropy [6, 7]. Therefore, the epitaxial strain offers the opportunities to tune both the macroscopic and microscopic properties of manganite films. While in the anisotropically-strained LCMO thin films deposited on (001)-oriented $NdGaO_3$ (NGO) substrate, multiple first-order transitions can be induced by a post-annealing process that greatly enhances the substrate coherency [8]. Here we report the magnetic images of the microscopic behaviors of a LCMO/NGO thin film using a home-built magnetic force microscope (MFM).

II. EXPERIMENTS

The sample we image is a 40 nm thick LCMO thin film deposited on NGO(001) substrate using pulsed laser deposition method. The growth details and more characterization can be found in Refs.[9−12]. The film suffers a strong anisotropic elastic epitaxial strain, which is compressive (−0.7%) and tensile (+0.85%) along the *a*- and *b*-axis, respectively [10]. The resistivity was measured on a quantum design physical property measurement system using the common four probe method.

The details of the home-build MFM are described in Ref.[13]. Briefly, the MFM is based on a home-designed approach motor (SpiderDrive) and is incorporated into a 20 T superconducting magnet. We use a piezoresistive cantilever (PRC400 from Hitachi High-Tech Science Corporation, Japan) as the force sensor. 5 nm Cr, 50 nm Co, and 5 nm Au are deposited to the one side of the pyramid-shape tip as the magnetic coatings. The tip was magnetized perpendicular to the cantilever prior to the measurements. We use the common frequency-modulated mode to image the magnetic signal using the

*Author to whom correspondence should be addressed. E-mail: qxl@ustc.edu.cn

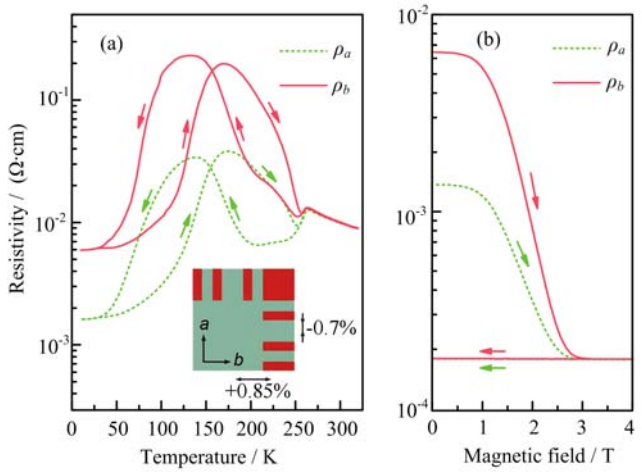

FIG. 1 (a) The temperature dependence of resistivity of the LCMO/NGO thin film with thickness of 45 nm. The temperature was firstly decreased to 10 K from room temperature and then warmed back to room temperature. The arrows indicate the sequences. The inset shows the configuration of the electrodes, along with the anisotropic epitaxial strain the film suffers from the substrate. a and b denotes the resistivity measured along a- and b-axis, respectively. (b) The field dependence of resistivity. A magnetic field along b-axis was applied after the sample was cooled down from room temperature.

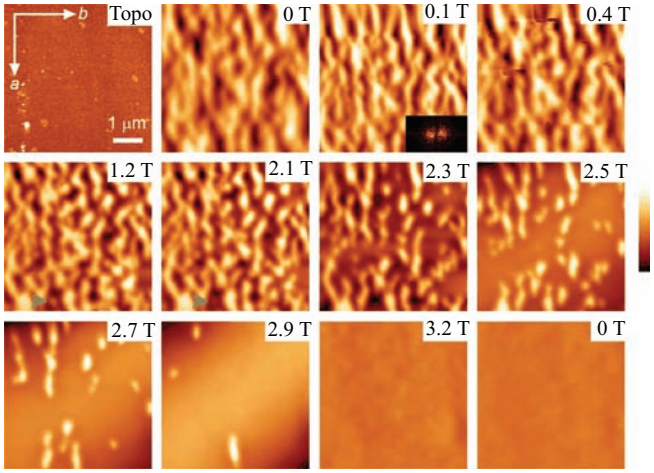

FIG. 2 The MFM images with increasing magnetic fields at 10 K. The magnetic field is applied perpendicularly to the sample surface. The size of all the images is 5 μm×5 μm. The color scale for these images is 40 nm (Topo), 3.5 Hz (0 T), 5.0 Hz (0.1 T), 6.2 Hz (0.4 T), 17.0 Hz (1.2−2.7 T), 12 Hz (2.9 T), 3.5 Hz (3.2−0 T). The crystalline axes are labeled in the topography image. The inset in the 0.1 T image is the fast Fourier transformation (FFT) image.

built-in phase-locked loop (PLL) in the R9 controller (RHK technology). The lift height of the tip is about 100 nm.

III. RESULTS

The temperature dependence of resistivity along the two in-plane crystalline axes in zero field of a 45 nm thick LCMO/NGO sample is shown in Fig.1(a). The large hysteresis with "∞" shape in the resistivity curve illustrates the incomplete first-order ferromagnetic metal (FM)-antiferromagnetic insulator (AFI) and AFI-FM transitions in addition to the higher paramagnetic-FM transition with Curie temperature T_C=260 K. Thus, the coexistence of AFI and FM phases is expected to be spanning the large temperature range below the FM-AFI transition at about 258 K. In addition, the resistivity measured along a-axis is apparently smaller than that measured along b-axis. The AFI phase will be melted if an external magnetic field is applied, as shown in Fig.1(b), where large drop in resistivity with increasing fields along both axes is observed. When the AFI phase is fully melted, the anisotropy in resistivity disappears. Thus, the anisotropy only exists in the phase-separated state and probably results from the anisotropic distribution of the phase domains.

The isothermal MFM images we obtained are shown in Fig.2. The temperature was stabilized at 10 K and the field was applied perpendicular to the sample surface. At this temperature, the sample is in the so-called frozen state, with a larger melting field compared to the FM dominated phase separation state [8]. The crystalline axes are labeled in the topography image. The MFM image shows there exist bright and dark stripes along a-axis even at 0 T. From 0.1 T to 1.2 T, the contrast is enhanced due to the magnetization of the FM phase domains, and the shape anisotropy is evidenced by the fast Fourier transformation (FFT) image in the inset of the 0.1 T image. The dark regions are ascribed to the FM phase since the attractive force between the FM phase domains and the tip causes a negative frequency shift in the resonant frequency of the cantilever. The percolation of FM phase can be clearly seen at 1.2 T, but it shall be noted that it already occurs at 0 T since the volume of the FM phase does not change until 2.1 T, where part of the bright regions transform into dark regions, as labeled by the grey arrow heads, suggesting the onset of melting of the AFI. When the field is further increased (2.3 T), the FM phase domains expand at the expense of the AFI phase counterparts. At 2.5 and 2.7 T, the AFI phase domains are reduced to fragments, with some short but stripe-like AFI domains left, whose size is further reduced with only several dots left (2.9 T), which resembles the magnetic bubble domains in some ferromagnetic films with strong perpendicular anisotropy [14], indicating potential applications in memory devices. The bright dots disappear totally at 3.2 T, leaving a homogenous and saturated FM phase. A notable characteristic is that these phase domains are unable to move. Then we reduce the field, but nearly no change is observed even when the field is decreased

DOI:10.1063/1674-0068/28/cjcp1504064

to zero, implying the AFI phase is a metastable phase at this temperature.

IV. DISCUSSION

In the MFM images, the coexistence of the AFI and FM phases in zero magnetic field is clearly observed. The anisotropic distribution of the phase domains can qualitatively account for the resistivity anisotropy. In addition, the melting process of the AFI phase is imaged. When increasing the magnetic field, we observed two processes. Firstly, the magnetization process of the FM phase domains is observed, evidenced by the enhancement of the signal contrast. Then at a higher field, the AFI phase begins to transform into FM phase, and eventually, the AFI domains disappear with a FM background left.

V. ACKNOWLEDGMENTS

This work was supported by the National Natural Science Foundation of China (No.U1232210, No.11374278, and No.11204306), the Project of Chinese National High Magnetic Field Facilities (No.Y46CLB1191B2), the Major Program of Development Foundation of Hefei Center for Physical Science and Technology (No.2014FXZY002), and the Scientific Research Grant of Hefei Science Center of Chinese Academy of Sciences.

[1] E. Dagotto, T. Hotta, and A. Moreo, Phys. Rep. **344**, 1 (2001).
[2] K. H. Ahn, T. Lookman, and A. R. Bishop, Nature **428**, 401 (2004).
[3] A. Biswas, M. Rajeswari, R. C. Srivastava, T. Venkatesan, R. L. Greene, Q. Lu, A. L. de Lozanne, and A. J. Millis, Phys. Rev. B **63**, 184424 (2001).
[4] M. Nakamura, Y. Ogimoto, H. Tamaru, M. Izumi, and K. Miyano, Appl. Phys. Lett. **86**, 182504 (2005).
[5] T. Jiang, S. Yang, H. Zhou, Y. Liu, W. Zhao, L. Feng, Y. Hou, Q. Lu, and X. Li, Appl. Phys. Lett. **104**, 203501 (2014).
[6] K. Lai, M. Nakamura, W. Kundhikanjana, M. Kawasaki, Y. Tokura, M. A. Kelly, and Z. X. Shen, Science **329**, 190 (2010).
[7] T. Z. Ward, J. D. Budai, Z. Gai, J. Z. Tischler, L. Yin, and J. Shen, Nat. Phys. **5**, 885 (2009).
[8] Z. Huang, L. F. Wang, X. L. Tan, P. F. Chen, G. Y. Gao, and W. B. Wu, J. Appl. Phys. **108**, 083912 (2010).
[9] L. F. Wang, X. L. Tan, P. F. Chen, B. W. Zhi, B. B. Chen, Z. Huang, G. Y. Gao, and W. B. Wu, AIP Adv. **3**, 052106 (2013).
[10] L. F. Wang, Z. Huang, X. L. Tan, P. F. Chen, B. W. Zhi, G. M. Li, and W. B. Wu, Appl. Phys. Lett. **97**, 242507 (2010).
[11] Z. Huang, G. Y. Gao, F. H. Zhang, X. X. Feng, L. Hu, X. R. Zhao, Y. P. Sun, and W. B. Wu, J. Magn. Magn. Mater. **322**, 3544 (2010).
[12] Z. Huang, G. Y. Gao, Z. Z. Yin, X. X. Feng, Y. Z. Chen, X. R. Zhao, J. R. Sun, and W. B. Wu, J. Appl. Phys. **105**, 113919 (2009).
[13] H. Zhou, Z. Wang, Y. Hou, and Q. Lu, Ultramicroscopy **147**, 133 (2014).
[14] A. Hubert and R. Schöfer, *in Magnetic Domains: the Analysis of Magnetic Microstructure*, Berlin: Springer, (1998).

DOI:10.1063/1674-0068/28/cjcp1504064